Transactions of the Materials Research Society of Japan 30[1] 87-92 (2005)

Bi_2MoO_6-BASED NATURAL-SUPERLATTICE OF BISMUTH-LAYER -STRUCTURED FERROELECRIC THIN FILMS

Akira Shibuya, Minoru Noda, Masanori Okuyama and Keisuke Saito*

Department of Systems Innovation, Graduate School of Engineering Science,

Osaka University, 1-3 Machikaneyama-cho, Toyonaka, Osaka 560-8531, Japan

Fax: 06-6850-6341, e-mail: shibuya@semi.ee.es.osaka-u.ac.jp

*BRUKER AXS K.K.,3-9-A Moriya-cho, Kanagawa-ku, Yokohama, Kanagawa 221-0022, Japan

Bi_2MoO_6 (BM) (m=1)-based natural-superlattice-structured BLSF thin films, which are Bi_2MoO_6–Bi_3TiNbO_9 (BM–BTN)(m=1–2) and Bi_2MoO_6–$Bi_4Ti_3O_{12}$ (BM–BIT) (m=1–3) have been prepared on $SrTiO_3$ (STO) (001) single crystal and $Pt/TiO_2/SiO_2/Si$ substrates by pulsed laser deposition (PLD) method. The c-lattice constant (6.73 nm) of the epitaxial BM–BTN (m=1–2) film on STO is very close to the value (6.54 nm) of the superlattice structure of one BM unit cell and two BTN unit cells. Polycrystalline BM–BTN (m=1–2) thin film on $Pt/TiO_2/SiO_2/Si$ substrate deposited at 450°C and post-annealed at 650°C shows long-range superlattice of 15.5 nm iterative layer which corresponds to 50 unit cells consisting of (113)-oriented BM (m=1) and (115)-oriented BTN (m=2). On the other hand, the c-lattice constant (2.47 nm) of BM–BIT (m=1–3) is very close to the value (2.45 nm) of the superlattice structure consisting of one-half BM (m=1) unit cell and one-half BIT (m=3) unit cell. This natural-superlattice structure consisting of non-sequential m number BLSF materials such as m=1 and 3 has never been reported so far. Therefore, the BM-based natural-superlattice structures have unique crystal properties different from conventional natural-superlattice structures.

Key words: Bi_2MoO_6, BLSF, ferroelectrics, natural superlattice

1. INTRODUCTION

Recently, natural-superlattice of bismath-layer-structured ferroelectric (BLSF) materials have attracted much interest as polarization enhancement is expected by structural modification of pseudo-perovskite layers through Bi_2O_2 layer [1-4]. This enhancement is preferable in their application for nonvolatile ferroelectric random access memory (FeRAM). The crystal structures of BLSF are generally formulated as $(Bi_2O_2)^{2+}$ $(A_{m-1}B_mO_{3m+1})^{2-}$, where m is the number of BO_6 octahedra in the pseudo-perovskite blocks (m=1 to 5). $Bi_4Ti_3O_{12}$–$SrBi_4Ti_4O_{15}$ (m=3–4) (BIT–SBTi) and Bi_3TiNbO_9–$Bi_4Ti_3O_{12}$ (m=2–3) (BTN–BIT) thin films are reported as natural-superlattice-structured BLSFs [2-5]. BIT–SBTi film prepared by a pulsed laser deposition (PLD) has the same superlattice structure as BIT–SBTi bulk ceramics which is 1–1 superlattice showing iteration of each unit cell layer [3], but in addition to 1–1 superlattice, BTN–BIT film has different superlattice structure which is 2–1 superlattice showing iteration of

one BTN and two BIT layers [4]. This 2–1 superlattice structure is different from that of BTN–BIT ceramics which has 1–1 superlattice structure. The 2–1 superlattice film shows good ferroelectric property due to the structural stress induced through Bi_2O_2 layer by the difference of lattice constants of pseudo-pervskite structures. The twice remanent polarization ($2P_r$) and twice coercive field ($2E_c$) of the BTN–BIT film are as large as 50 μC/cm^2 and 350 kV/cm, respectively.

In BLSF, the m number is smaller, the range of tolerance factor (t) for pseudo-pervskite units is wider. [5] In BLSF with m=1, there are no A-site ions in the pseudo-perovskite layer. From this viewpoint, natural-superlattice-structured BLSF with a small m number (m=1–2 and 1–3) are expected to have interesting crystalline properties and superior ferroelectric properties due to the large difference in lattice constants between BLSF materials with m=1 and m=2, or m=1 and m=3. Bi_2MoO_6 (BM) is selected as a m=1 BLSF material because BM is widely recognized not only as a ferroelectric material [6], but also as a catalyst for use in the selective oxidation [7].

In this study, we investigated Bi_2MoO_6–Bi_3TiNbO_9 (BM–BTN)(m=1–2) and Bi_2MoO_6–$Bi_4Ti_3O_{12}$ (BM–BIT) (m=1–3) thin films on $SrTiO_3$ (001) substrates and Pt/TiO_2/SiO_2/Si substrates prepared by PLD and oxygen annealing.

2. EXPERIMENTAL

The BM–BTN and BM–BIT pellets used as PLD targets were conventional ceramic disks prepared by solid-state reaction. The mixture of Bi_2O_3 (3% in excess of the stoichimetric composition because of its volatility), Nb_2O_5, TiO_2 and MoO_3 with a ratio of Bi:Nb:Ti:Mo= 5.15:1:1:1 and Bi:Ti:Mo= 6.18:3:1 were mixed by ball milling and pressed into pellets. After calcination at 800°C for 2 h, the pellets were ground, pressed into pellets, and sintered at 950°C for 1 h. BM–BTN and BM–BIT films were grown on $SrTiO_3$ (STO) (001) single-crystal and Pt(111)/TiO_2/SiO_2/Si substrates by PLD using ArF excimer laser (λ = 193 nm). The laser repetition rate was 5 Hz, the laser pulse energy density was 3.7 J/cm^2, the oxygen pressure was 0.07 Torr, and the substrates were heated from 400°C to 550°C. The thickness of the deposited films was approximately 400 nm. The BM–BTN films were post-annealed in O_2 for 45 min at 650°C. Finally, Pt electrodes were deposited on the BM–BTN films by rf sputtering at room temperature for electrical measurements. The crystalline structures were investigated by X-ray diffraction (XRD) analysis (CuKα radiation; λ = 0.1542 nm was used in this study). The polarization–electric field (P–E) hysteresis loops were evaluated using a ferroelectric test system with virtual ground circuitry (Toyo-technica, FCE-1) at 1 kHz.

3. RESULTS AND DISCUSSION

3.1 BM–BTN and BM–BIT bulk ceramic targets

Figure 1 shows XRD patterns of the (a) BM–BTN (m=1–2), (b) BM–BIT (m=1–3) ceramic targets. BM–BTN and BM–BIT, which include BM, don't have a natural-superlattice structure like Bi_2WO_6–Bi_3TiTaO_9 (m=1–2) ceramics [8] but have two phases of BM and, BTN or BIT. The main different behavior may be attributed to catalytic property of BM being markedly strong. BM is not only as a ferroelectric material [6], but also as a catalyst [7].

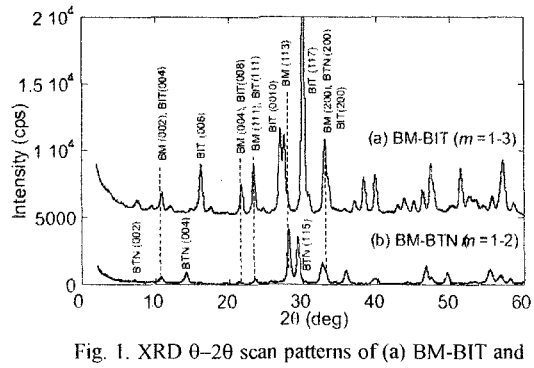

Fig. 1. XRD θ–2θ scan patterns of (a) BM-BIT and (b) BM-BTN ceramic targets.

Table. I. *a*, *b* and *c*-axis lattice constants of BM, BTN, BIT and BW-BTT ceramics.

	a	*b*	*c*
Bi_2MoO_6 (*m*=1)	0.552 nm	0.549 nm	1.624 nm
Bi_3TiNbO_9 (*m*=2)	0.540 nm	0.545 nm	2.516 nm
$Bi_4Ti_3O_{12}$ (*m*=3)	0.541 nm	0.545 nm	3.284 nm
Bi_2WO_6–Bi_3TiTaO_9 (*m*=1–2)ceramics	0.542 nm	0.540 nm	2.095 nm

Lattice constants of Bi_2MoO_6, Bi_3TiNbO_9, $Bi4Ti_3O_{12}$ and Bi_2WO_6–Bi_3TiTaO_9 are given in Table I.

3.2 *BM–BTN (m=1–2) thin films*

a) Epitaxial BM-BTN thin film on STO single-crystal substrate

An epitaxial BM–BTN thin film was prepared on an STO (001) single-crystal substrate by PLD at a substrate temperature of 550°C. Figure 2 shows the XRD pattern of the BM–BTN film on the STO (001) single-crystal substrate. BM–BTN film on STO (001) single-crystal substrate has different crystal property from the BM–BTN ceramic target. The BM–BTN film is almost of single phase and its *c*-lattice constant is estimated to be 6.738 nm taking into consideration the periodicity of the lattice structures. The lattice constant is very close to that (6.54 nm) of the superlattice structure consisting of one BM unit cell and two BTN unit cells, namely the 1–2 superlattice of BM–BTN. Also this half value (3.369 nm) of *c* lattice constant in the BM–BTN film is close to that (3.28 nm) of BIT (*m*=3). But it is difficult to consider that the BM–BTN film has (*m*=3) BLSF structure because of break of the charge neutrality such as $Bi_4TiNbMoO_{12}$ composition. That is why we expect that the BM–BTN film has 1–2 natural superlattice structure.

Figure 3 shows the XRD Debye cone of the BM–BTN film on the STO substrate obtained using a two-dimensional detector [D8 DISCOVER with GADDS, BRUKER AXS, INC.]. The broken lines are the

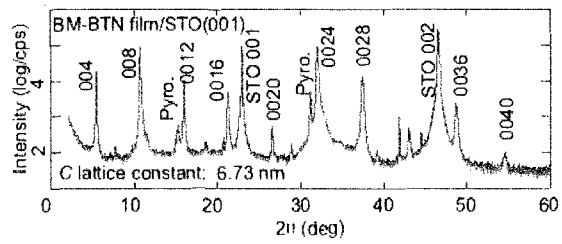

Fig. 2. XRD θ–2θ scan pattern of BM-BTN film on STO substrate at 550°C at oxygen pressure of 0.07 Torr.

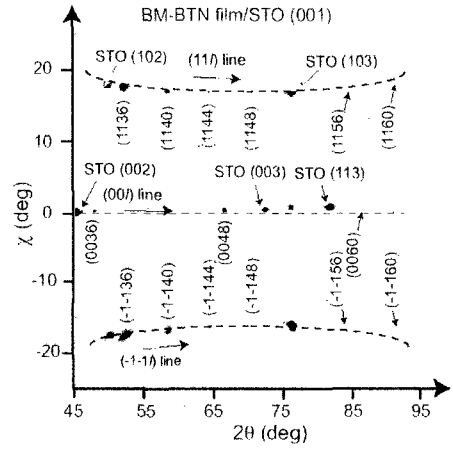

Fig. 3. XRD Debye cone of the epitaxial BM–BTN film on STO substrate obtained using two-dimensional detector.

interpolated curves of (11*l*), (00*l*) and (-1-1*l*) and clearly indicate that the BM–BTN film has an exact epitaxial BLSF structure along the *c*-axis. The lattice constants *a* (0.549 nm) and *b* (0.549 nm) were obtained from XRD reciprocal space mapping of the BM–BTN film.

b) Polycrystalline BM–BTN thin films on $Pt/TiO_2/SiO_2/Si$ substrate

The films deposited below 500°C consist mainly of (222)-oriented fluorite phase, and the films deposited at 550°C have a 1–2 superlattice of BM–BTN the same as the epitaxial BM–BTN film on the STO substrate which was described in 3.2. After fabricating Pt top electrodes, the ferroelectric properties of these films were measured. The films deposited at 450 and 500°C had very weak ferroelectricity as they did not show the BLSF phase but the fluorite phase, and the film deposited at 550°C was too leaky to be measured.

The oxygen post-annealing of the films of the fluorite phase deposited at around 500°C was carried out at 650°C for 45 min to improve their crystal and electric properties. The postannealing at 650°C makes these as-deposited BM–BTN films of fluorite phase changing drastically into BLSF phase. Usually, perovskite phase in BIT is recrystallized from pyrochlore or fluorite phase by annealing more than 800°C. But perovskite phase in BM–BTN is recrystallized from fluorite phase by as low as annealing at 650°C. This may be also attributed to catalytic property of BM.

These BLSF phases may have long-range superlattice structures consisting of BM (113) and BTN (115) as seen in the XRD patterns of the BM–BTN films in Fig. 4 because the films seem to have two satellite peaks which are the –1st and –2nd satellite peaks of the main peak of BM (113). The reason there are no +1st and +2nd satellite peaks is considered to be the superlattice structure being not perfect and uniform, but deformed. However, the definite reason for the one-side satellite peaks remains unclear. The long-range periodicity (Λ) of the superlattice is calculated from the diffraction angles of the main peak of BM (113) and the satellite peaks in Fig. 4 as follows,

$$\Lambda = \frac{(\mu - \nu)\lambda}{2(\sin\theta_\mu - \sin\theta_\nu)} \qquad (1)$$

Where μ and ν are the orders of a satellite peak (integer), θ_μ and θ_ν are the diffraction angle, and λ is the wavelength of X-ray [9]. The long-range periodicity (Λ) of the superlattice is estimated to be 15.5 nm, which corresponds to almost 50 BM (113) and BTN (115) layers.

However there is another assumption of these satellite-like peaks in Fig. 4 (c), which are attributed to the intermediate structures in BIT such as pyrochlore phase, $Bi_2Ti_2O_7$, and stacking-fault-induced structure as seen in recrystallized BIT from amorphous BIT [10].

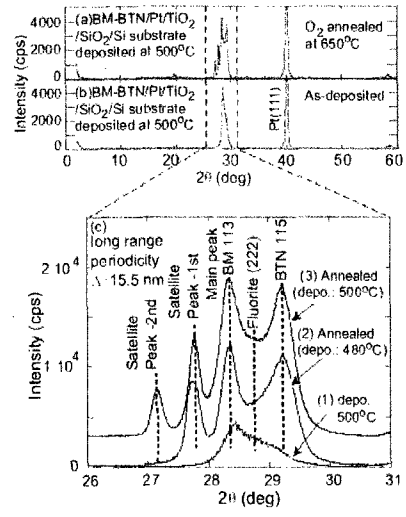

Fig. 4. XRD θ–2θ scan patterns of (a) post-annealed BM–BTN film deposited at 500°C, (b) as-deposited BM–BTN film deposited at 500°C. (c) detailed XRD profiles of (1) as-deposited BM–BTN film deposited at 500°C, (2) annealed BM–BTN films deposited at 480°C, and (3) annealed BM–BTN films deposited at 500°C on Pt(111)/TiO_2/SiO_2/Si substrates.

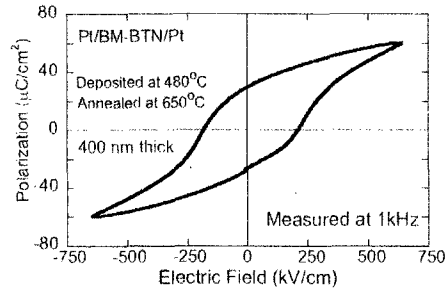

Fig. 5. *P-E* hysteresis loop of Pt/BM–BTN/Pt.

Among the polycrystalline BM–BTN films, the annealed film deposited at 480°C exhibits a good ferroelectric *P–E* hysteresis loop, as shown in Fig. 5. The *P–E* hysteresis loop shows that the twofold remanent polarization ($2P_r$) and twofold coercive field ($2E_c$) were 55 μC/cm^2 and 390 kV/cm, respectively. However, the saturation properties of the BM–BTN film suggest that the real $2P_r$ of the BM-BTN film can be estimated to be about 40 μC/cm^2.

3.3 BM–BIT (m=1–3) thin films

a) Epitaxial BM-BIT thin film on STO substrate

An epitaxial BM–BIT thin film was prepared on STO (001) single-crystal substrate by PLD as same as

(Received December 23, 2004; Accepted January 31, 2005)

BM–BTN film. Figure 6 shows the XRD pattern of the BM–BIT film on the STO substrate. The BM–BIT film seems to be almost single phase and its *c*-lattice constant is estimated to be 2.47 nm. The lattice constant is very close to that (2.45 nm) of the superlattice structure consisting of one BM unit cell and one BIT unit cell, namely 1–1 superlattice of BM–BIT. This natural-superlattice structure consisting of non-sequential *m* number BLSF materials such as m=1–3 has never been reported so far. Figure 7 shows the XRD of the BM-BIT thin film on STO substrate. The reciprocal space mapping suggests that the BM–BIT film has not only BM–BIT superlattice but also BM because of clear BM (113) peak. In Fig. 6, the 2θ of BM (002) peak is the same as BM–BIT (003) peak. The broken lines in Fig. 5 are the interpolated curves of (00*l*), (11*l*) and (22*l*) and clearly indicate that the film consisting of BM–BIT and BM has an exact epitaxial BLSF structure along the *c*-axis. The reason why there are both BM–BIT superlattice and BM in the epitaxial film is that twice *c* lattice constant of BM-BIT is almost the same as three times that of BM. Anyway it is noted that BM–BIT (m=1–3) superlattice can be prepared.

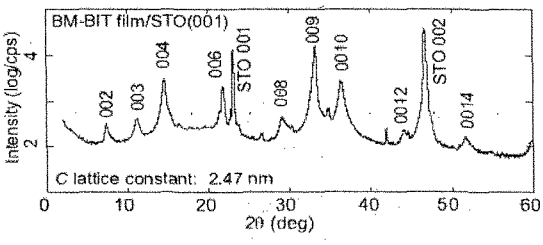

Fig. 6. XRD θ-2θ scan pattern of BM-BIT film on STO substrate at 550°C at oxygen pressure of 0.07 Torr.

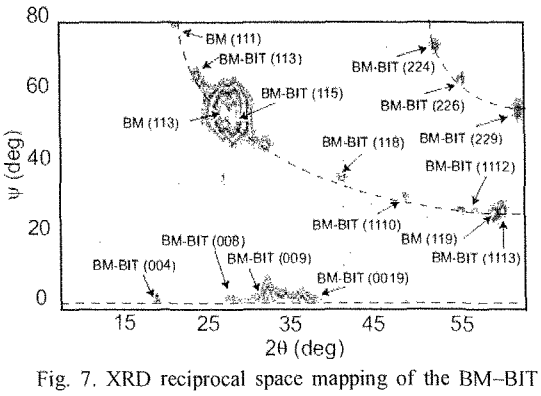

Fig. 7. XRD reciprocal space mapping of the BM–BIT film on STO (001) substrate.

b) Polycrystalline BM-BIT thin film on Pt/TiO_2/SiO_2/Si substrate

BM–BIT films were also deposited on Pt/TiO_2/SiO_2/Si substrates at substrate temperatures of 450°C with an oxygen pressure of 0.07 Torr and post-annealed at 650°C for 1h. Figure 8 shows the XRD patterns of (a) 650°C annealed BM–BIT film deposited at 450°C, (b) as-deposited BM–BIT film deposited at 450°C. As-deposited BM–BIT film has flurorite-like crystal property with the same manner of BM–BTN film. After oxygen annealing, the BM-BIT film has three kinds of phases which are BM, BIT and BM–BIT, respectively. The ferroelectricity of BM–BIT film is drastically improved after the annealing as seen in Fig. 9. $2P_r$ and $2E_c$ of the annealed BM–BIT film are 54 μC/cm^2 and 310 kV/cm, respectively. This good ferroelectricity may be attributed to many reasons. One reason is thought of structural stress by existing three kinds of phases in the films. Figure 10 shows SEM images of (a) BIT film and

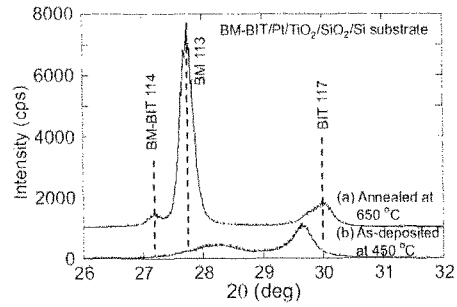

Fig. 8. θ-2θ scan patterns of (a) 650°C annealed BM–BIT film deposited at 450°C, (b) as-deposited BM–BIT film deposited at 450°C.

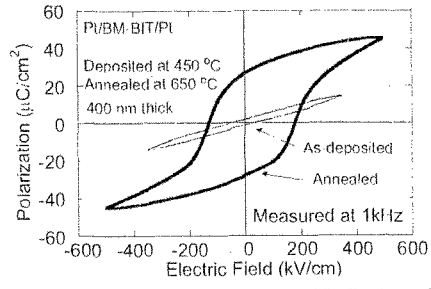

Fig. 9. *P-E* hysteresis loop of Pt/BM-BIT/Pt with and without the annealing.

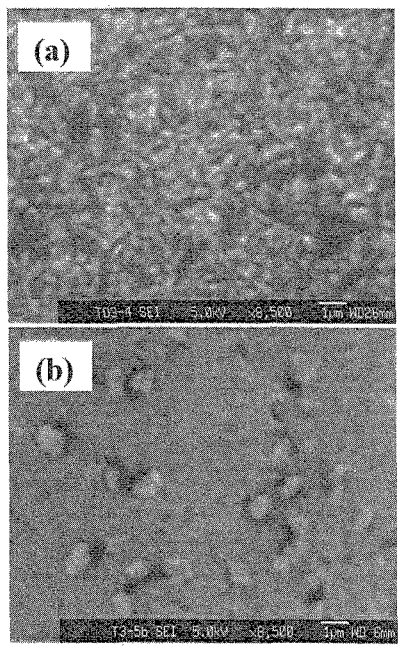

Fig. 10. SEM image of (a) BIT film and (b) BM-BIT film deposited at 450°C and post-annealed at 650°C.

(b) BM-BIT film deposited at 450°C and annealed at 650°C. Both films are prepared by the same condition, but the surface morphologies are quite different. The surface morphology of BIT film is very rough and the grain is typically plate-like. On the other hand, the surface of BM–BIT film is smooth in some locations and the grain is very large. From this point, catalytic BM induces BM–BIT to enlarge the large grain and domain structure during oxygen post-annealing. Those large clusters with large grain and domain structure are also one reason why annealed BM–BIT film has good ferroelectric property. These results imply that BM can assist crystallization of BM–BIT during the annealing after low temperature deposition. Polycrystalline BM–BIT films with good ferroelectric property have been prepared by appropriate process which has low deposition temperature as low as 450°C and oxygen post-annealing with catalytic BM material the same as in the BM–BTN thin fims. This preparation process is very effective for BM-based natural-superlattice structured BLSF material.

4. SUMMARY AND CONCLUSIONS

The natural-superlattice-structured BM-BTN film on STO (001) single crystal substrate have a 2–1 superlattice structure. Long-range natural-superlattice-structured BM–BTN thin films on $Pt/TiO_2/SiO_2/Si$ substrates are prepared by using PLD and oxygen post-annealing at 650°C. The long-range natural-superlattice-structured BM–BTN thin film shows good ferroelectricity with a $2P_r$ of 40 $\mu C/cm^2$. Also, natural-superlattice-structured BM–BIT films on STO(001) single crystal substrate are prepared. The polycrystalline BM–BIT film on $Pt/TiO_2/SiO_2/Si$ substrate deposited at 450°C and annealed at 650°C shows good ferroelectricity with a $2P_r$ of 54 $\mu C/cm^2$.

REFERENCES

[1] T. Kikuchi, A. Watanabe and K. Uchida, *Mater. Res. Bull.*, **12**, 299 (1977).

[2] Y. Noguchi, M. Miyayama and T. Kudo, *Appl. Phys. Lett.*, **77**, 3639 (2000).

[3] A. Shibuya, M. Noda, M. Okuyama, H. Fujisawa and M. Shimizu, *Appl. Phys. Lett.* **82**, 784 (2003).

[4] A. Shibuya, M. Noda and M. Okuyama, *Jpn. J. Appl. Phys.*, **42**, 5986 (2003).

[5] A. Shibuya, S. Ikemori, W. B. Wu, M. Noda and M. Okuyama, *Appl. Phys. Lett.*, **83**, 1411 (2003).

[6] I. H. Ismailzade, I. M. Aliyev, R. M. Ismailov, A. I. Alekberov *et al*, *Ferroelectrics* **22**, 853 (1979).

[7] D. J. Buttrey, T. Vogt, U. Wildgruber and W. R. Robinson, *J. Solid State Chem.*, **111**, 18 (1994).

[8] Y. Noguchi, R. Satoh, M. Miyayama and T. Kudo, *J. Cer. Soc. Jpn.*, **109**, 21 (2001).

[9] O. Nakagawara, T. Shimuta and T. Makino, S. Arai, *Appl. Phys. Lett.*, **77**, 3257 (2000).

[10] Y. Yoneda, J. Mizuki *et al.*, *Appl. Phys. Lett.*, **83**, 275 (2003).

(Received December 23, 2004; Accepted January 31, 2005)